Inorg. Chem. **2005**, *44*, 4215–4225

Cobalt(III) Carbonate and Bicarbonate Chelate Complexes of Tripodal Tetraamine Ligands Containing Pyridyl Donors: The Steric Basis for the Stability of Chelated Bicarbonate Complexes

Paul M. Jaffray, Lisa F. McClintock, Kay E. Baxter, and Allan G. Blackman*

Department of Chemistry, University of Otago, P. O. Box 56, Dunedin, New Zealand

Received December 12, 2004

The synthesis and characterization (X-ray crystallography, UV/vis spectroscopy, electrochemistry, ESI-MS, and ^{1}H, ^{13}C, and ^{59}Co NMR) of the complexes $[Co(L)(O_2CO)]ClO_4 \cdot xH_2O$ (L = tpa (tpa = tris(2-pyridylmethyl)amine) (x = 1), pmea (pmea = bis((2-pyridyl)methyl)-2-((2-pyridyl)ethyl)amine) (x = 0), pmap (pmap = bis(2-(2-pyridyl)ethyl)-(2-pyridylmethyl)amine) (x = 0), tepa (tepa = tris(2-(2-pyridyl)ethyl)amine) (x = 0)) which contain tripodal tetradentate pyridyl ligands and chelated carbonate ligands are reported. The complexes display different colors in both the solid state and solution, which can be rationalized in terms of the different ligand fields exerted by the tripodal ligands. Electrochemical data show that $[Co(tepa)(O_2CO)]^+$ is the easiest of the four complexes to reduce, and the variation in $E_{red.}$ values across the series of complexes can also be explained in terms of the different ligand fields exerted by the tripodal ligands, as can the ^{59}Co NMR data which show a chemical shift range of over 2000 ppm for the four complexes. $[Co(pmea)(O_2CO)]^+$ is fluxional in aqueous solution, and VT NMR spectroscopy (^{1}H and ^{13}C) in DMF-d_7 (DMF = dimethylformamide) over the temperature range −25.0 to 75.0 °C are consistent with inversion of the unique six-membered chelate ring. This process shows a substantial activation barrier ($\Delta G^{\ddagger}$ = 58 kJ mol^{-1}). The crystal structures of $[Co(tpa)(O_2CO)]ClO_4 \cdot H_2O$, $[Co(pmea)(O_2CO)]ClO_4 \cdot 3H_2O$, $[Co(pmap)(O_2CO)]ClO_4$, and $[Co(tepa)(O_2CO)]ClO_4$ are reported, and the complexes containing the asymmetric tripodal ligands pmea and pmap both crystallize as the 6-isomer. The carbonate complexes all show remarkable stability in 6 M HCl solution, with $[Co(pmap)(O_2CO)]^+$ showing essentially no change in its UV/vis spectrum over 4 h in this medium. The chelated bicarbonate complexes $[Co(pmea)(O_2COH)]ZnCl_4$, $[Co(pmap)(O_2COH)][Co(pmap)(O_2CO)](ClO_4)_3$, $[Co(pmap)(O_2COH)]ZnCl_4 \cdot H_2O$, and $[Co(pmap(O_2COH)]ZnBr_4 \cdot 2H_2O$ can be isolated from acidic aqueous solution, and the crystal structure of $[Co(pmap)(O_2COH)]ZnCl_4 \cdot 3H_2O$ is reported. The stability of the carbonate complexes in acid is explained by analysis of the crystallographic data for these, and other slow to hydrolyze chelated carbonate complexes, which show that the *endo* (coordinated) oxygen atoms are significantly hindered by atoms on the ancillary ligands, in contrast to complexes such as $[Co(L)(O_2CO)]^+$ (L = $(NH_3)_4$, $(en)_2$, tren, and nta), which undergo rapid acid hydrolysis and which show no such steric hindrance.

Introduction

Co(III) complexes containing the chelated carbonate ligand have been known since the time of Werner[1] and have proven useful as starting materials for the synthesis of numerous Co(III) complexes due to the usual acid lability of the carbonate ligand. Treatment of complexes such as $Na_3[Co(O_2CO)_3] \cdot 3H_2O$ [2] and $[Co(en)_2(O_2CO)]ClO_4$ with acid in a weakly coordinating solvent generally results in rapid evolution of CO_2 and production of a solvento intermediate which can then react relatively rapidly with an entering ligand of choice. The kinetics of acid-catalyzed hydrolysis reactions of chelated carbonate Co(III) complexes have been extensively studied over many years,[3−12] and it has been shown

* E-mail: blackman@alkali.otago.ac.nz. FAX: +64 3 4797906.

(1) Jursík, F.; Kaufmann, G. B. In *Coordination Chemistry: A Century of Progress*; Kaufmann, G. B., Ed.; ACS Symposium Series 565; American Chemical Society: Washington, D.C., 1994; Chapter 4, p 63.
(2) Bauer, H. F.; Drinkard, W. C. *Inorg. Synth.* **1966**, *8*, 202−204.
(3) Scheidegger, H.; Schwarzenbach, G. *Chimia* **1965**, *19*, 166−169.
(4) Jordan, R. B.; Francis, D. J. *Inorg. Chem.* **1967**, *6*, 1605−1606.
(5) Sastri, V. S.; Harris, G. M. *J. Am. Chem. Soc.* **1970**, *92*, 2943−2946.
(6) Harris, G. M.; Hyde, K. E. *Inorg. Chem.* **1978**, *17*, 1892−1896.

10.1021/ic0482537 CCC: $30.25
Published on Web 05/06/2005

that the rates of such reactions, while usually rapid, are critically dependent on the nature of the ancillary ligand(s) about the Co(III) center; Buckingham and Clark's definitive study found rate variations of at least 7 orders of magnitude for Co(III) complexes containing a single chelated carbonate ligand.[13] Despite this large range of rates, even the slowest acid hydrolysis reaction of those studied in this paper is still relatively rapid, with a half-life for chelate ring-opening of $[Co(N\text{-mecyclen})(O_2CO)]^+$ (*N*-mecyclen = 1-methyl-1,4,7,-10-tetraazacyclododecane) of about 300 s at $[H_3O]^+ = 1.0$ M. However, the analogous reactions for Co(III) carbonate complexes containing pyridyl-based ligands have been shown to be significantly slower than this. Springborg and Schäffer[14] were the first to show that the $[Co(py)_4(O_2CO)]^+$ ion is extraordinarily resistant to acid-catalyzed hydrolysis, and the extreme inertness of cobalt(III) carbonate complexes containing pyridyl donor ligands was later further demonstrated by the protonation of $[Co(tepa)(O_2CO)]ClO_4$ (tepa = tris(2-(2-pyridyl)ethyl)amine) in aqueous acidic solution to give the chelated bicarbonate complex $[Co(tepa)(O_2COH)](ClO_4)_2 \cdot 3H_2O$, which has been characterized by X-ray crystallography.[15] Since this report, a number of other chelated bicarbonate species containing Ir(III),[16,17] Cu(II),[18] Co(III),[19] and Zr(IV)[20] have been structurally characterized[21] but such species are still rare, and the reasons for their stability have yet to be fully ascertained. In this paper, we report the synthesis and structural characterization of cobalt(III) carbonate and bicarbonate chelate complexes of tepa, pmap (pmap = bis(2-(2-pyridyl)ethyl)(2-pyridylmethyl)amine), pmea (pmea = bis((2-pyridyl)methyl)-2-((2-pyridyl)ethyl)-amine), and tpa (tpa = tris(2-pyridylmethyl)amine) (Figure 1). These ligands form a homologous series and thus allow an opportunity to investigate the effects of small structural changes in the ligands on the structural, spectral, electrochemical, and NMR properties of the resulting metal complexes. We show in this paper that such effects are surprisingly large. We also provide structural evidence that supports the proposal that the stability of the carbonate complexes toward acid is due to the sterically hindered nature of the *endo* (coordinated) oxygen atoms of the chelated carbonate ligand.

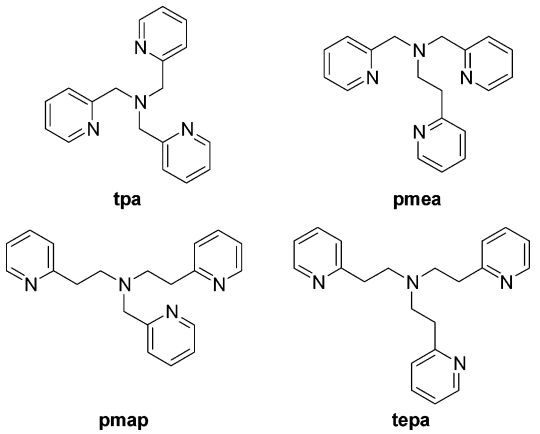

Figure 1. Structures of the tripodal amine ligands.

Experimental Section

General Methods. Elemental analyses were performed by the Campbell Microanalytical Laboratory, University of Otago. Routine ^1H and ^{13}C NMR spectra were recorded in D_2O on a Varian VXR 300 MHz spectrometer at ambient temperature. Variable-temperature ^1H and ^{13}C NMR spectra were recorded in DMF-d_7 on a Varian Europa 500 MHz spectrometer operating at 499.743 and 125.672 MHz, respectively, and chemical shifts are reported relative to residual solvent signals at 25.0 °C. ^{59}Co NMR spectra were recorded on the same instrument in a 10 mm NMR tube at either 119.500 MHz ($[Co(tpa)(O_2CO)]^+$, $[Co(pmea)(O_2CO)]^+$, and $[Co(pmap)(O_2CO)]^+$ complexes) or 119.750 MHz ($[Co(tepa)(O_2CO)]^+$ complex), and chemical shifts are reported relative to an external reference of $K_3[Co(CN)_6]$ (0 ppm). UV−vis spectra were recorded on a Varian Cary 500 Scan UV−vis−near-IR spectrophotometer thermostated at 25.0 °C. Electrospray mass spectra were obtained on a Shimadzu LCMS-QP8000α system using direct injection via a manual Rheodyne injector. Positive ionization techniques were used on an ESI probe (90/10 MeCN/H_2O mobile phase, 0.2 mL min^{-1}; CDL temperature, 250 °C; 4.5 kV). Electrochemical data were recorded on an EG&G PAR Model 273A Potentiostat with Model 270 software. Cyclic voltammograms were recorded from nitrogen-purged 0.5 mM acetonitrile solutions with 0.1 M tetrabutylammonium perchlorate as the supporting electrolyte. The electrochemical cell consisted of a 1.6 mm diameter platinum working electrode embedded in a KeL-F cylinder with a platinum auxiliary electrode and a saturated potassium chloride/calomel reference electrode. $E_{red.}$ values are reported relative to the decamethylferrocenium/decamethylferrocene couple.

Syntheses. All materials were LR grade or better and were used as received, and all syntheses were carried out under aerobic conditions. The tripodal tetraamine ligands tepa,[22] pmap, pmea,[23]

(7) Cooper, J. N. *J. Chem. Educ.* **1980**, *57*, 823−824.
(8) van Eldik, R.; Harris, G. M. *Inorg. Chim. Acta* **1983**, *70*, 147−149.
(9) van Eldik, R.; Spitzer, U. *Trans. Met. Chem.* **1983**, *8*, 351−354.
(10) Buckingham, D. A.; Clark, C. R. *Inorg. Chem.* **1993**, *32*, 5405−5407.
(11) Massoud, S. S.; Jordan, R. B. *Inorg. Chim. Acta* **1994**, *221*, 9−15.
(12) Kitamura, Y.; Yano, L.; Fujimori, K.; Mizuki, R.; Hayashi, M.; Shibata, A. *Bull Chem. Soc. Jpn.* **2000**, *73*, 2025−2032.
(13) Buckingham, D. A.; Clark, C. R. *Inorg. Chem.* **1994**, *33*, 6171−6179.
(14) Springborg, J.; Schäffer, C. E. *Acta Chem. Scand.* **1973**, *27*, 3312−3322.
(15) Baxter, K. E.; Hanton, L. R.; Simpson, J.; Vincent, B. R.; Blackman, A. G. *Inorg. Chem.* **1995**, *34*, 2795−2796.
(16) McLoughlin, M. A.; Keder, N. L.; Harrison, W. T. A.; Flesher, R. J.; Mayer, H. A.; Kaska, W. C. *Inorg. Chem.* **1999**, *38*, 3223−3227.
(17) Lee, D. W.; Jensen, C. M.; Morales-Morales, D. *Organometallics* **2003**, *22*, 4744−4749.
(18) Mao, Z.-W.; Liehr, G.; van Eldik, R. *J. Am. Chem. Soc.* **2000**, *122*, 4839−4840.
(19) Broge, L.; Sotofte, I.; Olsen, C. E.; Springborg, J. *Inorg. Chem.* **2001**, *40*, 3124−3129.
(20) Tutass, A.; Klopfer, M.; Huckstadt, H.; Cornelissen, U.; Homborg, H. *Z. Anorg. Allg. Chem.* **2002**, *628*, 1027−1044.
(21) In our original publication describing the synthesis of $[Co(tepa)(O_2COH)](ClO_4)_2 \cdot 3H_2O$, two references detailing structurally characterized chelating bicarbonate species containing Co(II) and Cd(II) were inadvertently omitted; see (for Co(II) and Cd(II), respectively): Doering, M.; Meinert, M.; Uhlig, E.; Dahlenburg, L.; Fawzi, R. *Z. Anorg. Allg. Chem.* **1991**, *598*−*599*, 71−82. Ito, H.; Ito, T. *Acta Crystallogr.* **1985**, *C41*, 1598−1602.
(22) Brownstein, S. K.; Plouffe, P.-Y.; Bensimon, C.; Tse, J. *Inorg. Chem.* **1994**, *33*, 354−358.
(23) Schatz, M.; Becker, M.; Thaler, F.; Hampel, F.; Schindler, S.; Jacobson, R. R.; Tyeklar, Z.; Murthy, N. N.; Ghosh, P.; Chen, Q.; Zubieta, J.; Karlin, K. D. *Inorg. Chem.* **2001**, *40*, 2312−2322. Note that prior alternative syntheses of pmea (Højland, F.; Toftlund, H.; Yde-Andersen, S. *Acta Chem. Scand., Ser. A* **1983**, *37*, 251−257) and pmap (Dietrich, J.; Heinemann, F. W.; Schrodt, A.; Schindler, S. *Inorg. Chim. Acta* **1999**, *288*, 206−209) are also available.

and tpa[24] and the complexes $Na_3[Co(O_2CO)_3]\cdot 3H_2O$ [2] and $[Co(tepa)(O_2CO)]ClO_4$ [15] were prepared as previously described. The free-base pmap ligand was converted to the tetrahydrobromide salt by addition of 2 M HBr to the free-base ligand, removal of solvent and crystallization from boiling ethanol.

CAUTION! Although we have experienced no problems with the perchlorate salts described herein, they should at all times be treated as potentially explosive and handled accordingly.

$[Co(tepa)(O_2CO)]ClO_4$. The synthesis of this complex has been reported previously, but full characterization details were not included.[15] ^{1}H NMR (D_2O): δ 9.54 (1H, d), 8.51 (2H, d), 7.95 (4H, m), 7.41 (5H, m), 3.83 (3H, m), 3.62 (3H, m), 3.48 (2H, t), 3.21 (2H, m), 3.04 (2H, m).^{13}C NMR (D_2O): δ 166.5, 163.1, 163.0, 152.8, 152.0, 141.6, 141.2, 128.5, 127.7, 126.9, 124.6, 55.4, 53.6, 31.9, 31.5. UV−vis (λ_{max}(H_2O), nm (ϵ, $M^{-1}cm^{-1}$)): 526 (102), 384 (163).

$[Co(pmap)(O_2CO)]ClO_4$. Pmap.4HBr (2.00 g, 3.12 mmol) was added to a suspension of $Na_3[Co(O_2CO)_3]\cdot 3H_2O$ (1.30 g, 3.59 mmol) in H_2O (20 mL). The mixture was heated at 65 °C for 5 min and then filtered to give a red-purple solution which was diluted to ∼600 mL and loaded onto Sephadex SP-C25 cation-exchange resin. Elution with 0.1 M $NaClO_4$(aq) removed a pink band which yielded microcrystals on a concentration of the eluate to low volume (rotavap). These were removed by filtration, washed with ice cold water and 2-propanol, and recrystallized from hot water (70 °C) to give $[Co(pmap)(O_2CO)]ClO_4$ (1.40 g, 73% based on Co). Anal. Calcd for $CoC_{21}H_{22}N_4O_7Cl$: C, 46.98; H, 4.13; N, 10.44; Cl, 6.60. Found: C, 47.14; H, 4.20; N, 10.48; Cl, 6.66. ESI-MS. Calcd for $[CoC_{21}H_{22}N_4O_3]^+$: 437. Found: 437. UV−vis (λ_{max}(H_2O), nm (ϵ, M^{-1} cm^{-1})): 515 (140), 360 (189).^{1}H NMR (D_2O): δ 9.26 (1H, d), 8.71 (1H, d), 8.14 (1H, t), 8.04 (2H, m), 7.82 (3H, m), 7.67 (2H, m), 7.35 (2H, m), 5.18 (1H, d), 4.50 (1H, d), 3.84 (1H, m), 3.53 (2H, m), 3.07 (2H, m), 2.76−2.93 (3H, m). ^{13}C NMR (D_2O): δ 168.5, 165.8, 164.7, 162.4, 155.3, 152.8, 152.6, 144.2, 143.8, 143.7, 129.9, 129.5, 129.0, 128.7, 127.2, 126.3, 69.5, 58.9, 57.5, 35.9, 34.2.

$[Co(pmea)(O_2CO)]ClO_4$. A solution of pmea (1.07 g, 3.52 mmol) in 1/1 water/methanol (17 mL) was added to $[Co(H_2O)_6](ClO_4)_2$ (1.30 g, 4.27 mmol) in H_2O (17 mL). To this were added $NaHCO_3$ (0.30 g, 3.57 mmol) and PbO_2 (1.20 g, 5.02 mmol), and the resulting suspension was stirred overnight at room temperature and then filtered through Celite to give a red/orange solution. This was diluted with water to ∼600 mL and loaded onto Sephadex SP C-25 cation-exchange resin. Elution with 0.1 M $NaClO_4$(aq) removed a red/orange band which yielded the product as a microcrystalline material on the concentration of the eluate to low volume (rotavap). The product was removed by filtration, washed with 2-propanol and ether, and then recrystallized from hot water (70 °C) to give $[Co(pmea)(O_2CO)]ClO_4$ as chunky red crystals (1.1 g, 49% based on Co). Anal. Calcd for $CoC_{20}H_{20}N_4O_7Cl$: C, 45.95; H, 3.86; N, 10.72; Cl, 6.78. Found: C, 45.70; H, 3.94; N, 10.68; Cl, 6.81. ESI-MS. Calcd for $CoC_{20}H_{20}N_4O_3^+$: 423. Found: 423. UV−vis (λ_{max}(H_2O), nm (ϵ, M^{-1} cm^{-1})): 500 (180), 357 (209). ^{1}H NMR (DMF-d_7, −25.0 °C): δ 9.44 (1H, d), 8.82 (1H, d), 8.22 (2H, t), 8.11 (1H, t), 8.08 (1H, d), 7.87 (2H, t), 7.81 (1H, d), 7.26 (1H, t), 7.60 (1H, t), 7.49 (1H, d), 5.56 (1H, d), 5.30 (2H, d), 5.10 (1H, d), 3.75 (1H, d), 3.34 (1H, d), 3.20 (1H, t), 2.60 (1H, t). ^{13}C NMR (DMF-d_7, −25.0 °C): δ 166.7, 164.3, 164.0, 162.1, 151.9, 151.1, 150.3, 142.1, 141.8, 140.9, 128.0, 126.9, 126.6, 126.0, 124.4, 122.2, 67.9, 66.5, 57.2, 32.5. X-ray crystallographic analysis showed the complex to exist as a trihydrate, and complete desolvation occurs on drying.

$[Co(tpa)(O_2CO)]ClO_4\cdot H_2O$. Tpa.3HBr (4.70 g, 8.82 mmol) was added to a suspension of $Na_3[Co(O_2CO)_3]\cdot 3H_2O$ (3.66 g, 10.1 mmol) in H_2O (60 mL). The mixture was heated at 65 °C for 5 min and then filtered, and the resulting brown/orange filtrate was diluted to 1000 mL and loaded onto a Sephadex SP-C25 cation-exchange column. Elution with 0.1 M $NaClO_4$(aq) removed an orange band, and concentration of the eluate to low volume (rotavap) gave the microcrystalline product. This was removed by filtration and washed with minimal amounts of ice cold water and 2-propanol. Recrystallization from hot water (70 °C) gave $[Co(tpa)(O_2CO)]ClO_4\cdot H_2O$ as an orange-brown solid (1.35 g, 25%). Anal. Calcd for $CoC_{19}H_{20}N_4O_8Cl$: C, 43.32; H, 3.83; N, 10.64; Cl, 6.73. Found: C, 43.41; H, 3.66; N, 10.71; Cl, 6.85. ESI-MS. Calcd for $CoC_{19}H_{18}N_4O_3^+$: 409. Found: 409. UV−vis (λ_{max}(H_2O), nm (ϵ, $M^{-1}cm^{-1}$)): 487 (192), 348 (200). ^{1}H NMR (D_2O): δ 8.90 (1H, d), 8.55 (2H, d), 8.11 (2H, t), 7.90 (1H, t), 7.72 (2H, d), 7.64 (3H, m), 7.31 (1H, d), 5.37 (2H, d), 5.18 (4H, m). ^{13}C NMR (D_2O): δ 169.0, 165.4, 164.6, 152.6, 151.7, 144.5, 143.5, 129.8, 129.7, 126.5, 124.8, 72.3, 72.0. The synthesis of this complex as the PF_6^- salt has been reported previously.[25]

$[Co(pmea)(O_2COH)]ZnCl_4$. An aqueous solution of $[Co(pmea)(O_2CO)]ClO_4$ (0.038 M, 10.0 mL) was treated with an equivalent volume of 2 M $ZnCl_2$ in 5 M HCl. Pink crystals deposited on storage at 4 °C for 24 h. The crystals were filtered, washed with ice cold water, and dried in air to give $[Co(pmea)(O_2COH)]ZnCl_4$ (0.11 g, 46%). Anal. Calcd for $CoC_{20}H_{21}N_4O_3Cl_4Zn$: C, 38.03; H, 3.35; N, 8.87; Cl, 22.45. Found: C, 37.84; H, 3.40; N, 8.63; Cl, 21.10.

$[Co(pmap)(O_2COH)][Co(pmap)(O_2CO)](ClO_4)_3$. Aqueous solutions of $HClO_4$ (5.4 M, 2.0 mL) and $NaClO_4$ (5.4 M, 1.0 mL) were added to an aqueous solution of $[Co(pmap)(O_2CO)]ClO_4$ (0.026 M, 3.0 mL). Purple crystals of sufficient quality for X-ray structural determination deposited on storage at 4 °C for 24 h. The crystals were filtered and washed with minimal volumes of water and 2-propanol. The product was air-dried to give $[Co(pmap)(O_2COH)][Co(pmap)(O_2CO)](ClO_4)_3$ (0.032 g, 70%). Anal. Calcd for $Co_2C_{42}H_{45}N_8O_{18}Cl_3$: C, 42.96; H, 3.86; N, 9.55; Cl, 9.06. Found: C, 43.12; H, 3.73; N, 9.54; Cl, 8.99.

$[Co(pmap)(O_2COH)]ZnCl_4\cdot H_2O$. An aqueous solution of $[Co(pmap)(O_2CO)]ClO_4$ (0.026 M, 20 mL) was treated with an equivalent volume of 2 M $ZnCl_2$ in 5 M HCl. Purple crystals of sufficient quality for X-ray structural determination deposited on storage at 4 °C for 48 h, and these were filtered, then washed with small volumes of 2-propanol and ether. The product was dried in air to give $[Co(pmap)(O_2COH)]ZnCl_4\cdot H_2O$ (0.142 g, 42%). Anal. Calcd for $CoC_{21}H_{25}N_4O_4Cl_4Zn$: C, 38.01; H, 3.80; N, 8.45; Cl, 21.37. Found: C, 37.99; H, 4.07; N, 8.37; Cl, 21.38. X-ray crystallographic analysis showed the complex to exist as a trihydrate, and partial desolvation occurs on drying.

$[Co(pmap)(O_2COH)]ZnBr_4\cdot 2H_2O$. An aqueous solution of $[Co(pmap)(O_2CO)]ClO_4$ (0.026 M, 2.0 mL) was treated with an equivalent volume of 2 M $ZnBr_2$ in 5 M HBr. Storage at 4 °C for 24 h resulted in precipitation of a purple solid, which was filtered and washed with minimal volumes of 2-propanol and ether. The product was dried in air to give $[Co(pmap)(O_2COH)]ZnBr_4\cdot 2H_2O$ (0.037 g, 83%). Anal. Calcd for $CoC_{21}H_{27}N_4O_5Br_4Zn$: C 29.35; H, 3.17; N, 6.52; Br, 37.19. Found: C, 29.49; H, 2.93; N, 6.61; Br, 37.04.

(24) Canary, J. W.; Wang, Y.; Roy, R., Jr.; Que, L., Jr.; Miyake, H. *Inorg. Synth.* **1998**, *32*, 70−75.

(25) Dalgaard, P.; McKenzie, C. J. *J. Mass Spectrom.* **1999**, *34*, 1033−1039.

X-ray Crystallography. X-ray data were collected at low temperature on a Siemens SMART system using graphite-monochromated Mo Kα radiation with exposures over 0.3° and were corrected for Lorentz and polarization effects using SAINT.[26] All structures were solved using SIR-97[27] running within the WinGX package,[28] and weighted full-matrix refinement on F^2 was carried out using SHELXL-97.[29] Hydrogen atoms were included in calculated positions and were refined as riding atoms with individual (or group, if appropriate) isotropic displacement parameters. Rotational disorder in the ClO_4^- anion of $[Co(pmap)(O_2CO)]ClO_4$ was evidenced by large thermal parameters, and the anion was thus modeled as two separate tetrahedra of O atoms about the same Cl atom, with a 54:46 occupancy. Two water O atoms in $[Co(pmea)(O_2CO)]ClO_4 \cdot 3H_2O$ were found to be disordered over three sites, with site occupancy factors for the three positions of 0.8, 0.7, and 0.5. Hydrogen atoms of the lattice water molecules in this complex, $[Co(tpa)(O_2CO)]ClO_4 \cdot H_2O$ and $[Co(pmap)(O_2COH)]ZnCl_4 \cdot 3H_2O$ could not be located in a search of the Fourier map and were thus not included in the refinement. The bicarbonate proton in $[Co(pmap)(O_2COH)]ZnCl_4 \cdot 3H_2O$ was located in a careful search of the Fourier map and was included in the final refinement cycles. It should be noted that the structures of $[Co(tpa)(O_2CO)]ClO_4 \cdot H_2O$ and $[Co(pmap)(O_2COH)]ZnCl_4 \cdot 3H_2O$ are of significantly poorer quality than the other three structures reported herein, as can be seen by their comparatively high R factors, and bond length and angle data for these structures should be analyzed with caution. We believe that this is a consequence of the poor quality of the platelike crystals obtained for these two complexes, as evidenced by the high R_{int} and R_{sigma} values (0.1313, 0.2569 and 0.2267, 0.2146 respectively). Despite numerous attempts, we found it impossible to grow better quality crystals. While solutions of both structures were easily obtained, some problems were experienced in their refinements. A single ISOR restraint was required to stop C25 displaying nonpositive definite thermal parameters in $[Co(tpa)(O_2CO)]ClO_4 \cdot H_2O$, while the C21−O3 distance in $[Co(pmap)(O_2COH)]ZnCl_4 \cdot 3H_2O$ was restrained to 1.26 Å to stop its reduction to nonsensical values during refinement.

Results and Discussion

Carbonate Complexes. While Co(III) complexes of amine ligands are generally prepared by air oxidation of a Co(II) salt in the presence of the free-base ligand, this method proved ineffective for the synthesis of complexes containing the pyridyl tripodal ligands tepa and pmap. In fact, an aqueous solution containing $[Co(H_2O)_6](ClO_4)_2$ and tepa is, quite remarkably, completely resistant to air oxidation, remaining pale pink even on prolonged bubbling of air through the solution. Thus $[Co(pmea)(O_2CO)]ClO_4$ and $[Co(tepa)(O_2CO)]ClO_4$ were prepared by PbO_2 oxidation of a solution (H_2O/MeOH) of the free-base ligand, $[Co(H_2O)_6](ClO_4)_2$ and $NaHCO_3$, while $[Co(pmap)(O_2CO)]ClO_4$ and $[Co(tpa)(O_2CO)]ClO_4 \cdot H_2O$ were prepared by reaction of the hydrobromide salt of the ligand with $Na_3[Co(O_2CO)_3] \cdot 3H_2O$ in aqueous solution. In all cases purification was effected by chromatography on Sephadex cation-exchange resin and the complexes were obtained in good yield following crystallization as the perchlorate salts.

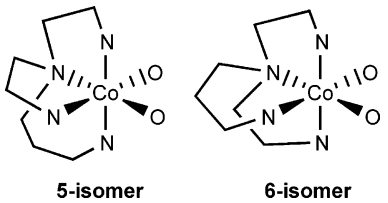

Figure 2. Geometric isomeric possibilities for six-coordinate complexes containing asymmetric tripodal ligands. 5- and 6-isomer refer to the size of the chelate ring in the same plane as the carbonate ligand.[31,57]

The low symmetries of the pmap and pmea ligands mean that geometric isomeric possibilities exist for $[Co(pmea)(O_2CO)]ClO_4$ and $[Co(pmap)(O_2CO)]ClO_4$, with both potentially able to exist as either 5- or 6-isomers (Figure 2). Observation of 20 peaks due to the pmap ligand in the ^{13}C NMR spectrum of $[Co(pmap)(O_2CO)]ClO_4$ suggested the presence of only the 6-isomer in solution, and this isomer was also observed in the crystal structure (see below). However, both ^1H and ^{13}C NMR spectroscopies showed that $[Co(pmea)(O_2CO)]ClO_4$ exists as an isomeric mixture of the 5- and 6-isomers in solution, with the 6-isomer predominating. Multiple recrystallizations failed to result in an isomerically pure product (11% of the 5-isomer remained after six recrystallizations) and passage down a 3 m Sephadex column eluted with sodium *p*-toluenesulfonate[30] also failed to separate the isomers. Although the crystal structure of $[Co(pmea)(O_2CO)]ClO_4$ shows the presence of the 6-isomer only, we are still not certain whether the solid material is a mixture of the two isomers, or whether equilibration between the two isomers takes place on dissolution of the pure 6-isomer in water as has been observed previously in $[Co(abap)(OH_2)_2]^{3+}$ (abap = (2-aminoethyl)bis(3-aminopropyl)-amine).[31] Arguing against the latter is the fact that the presence of the tripodal ligand presumably precludes an intramolecular Bailar or Ray-Dutt twist isomerization mechanism, and thus isomerization would require either Co−N or Co−O bond breaking and hence formation of some detectable aqua species. However, VT NMR studies in DMF-d_7 (see below) show that the isomeric ratio changes as the temperature is increased to 75 °C, and this strongly suggests that isomerization is in fact occurring. In this respect, it is interesting to note that the complex $[Co(baep)(O_2CO)]ClO_4$, where baep (baep = (3-aminopropyl)bis(2-aminoethyl)-amine) is the aliphatic congener of pmea, crystallizes as the 5-isomer.[32]

^1H and ^{13}C NMR data for $[Co(pmea)(O_2CO)]ClO_4$ give evidence for unexpected rigidity of the six-membered chelate ring in this complex. The ^1H NMR spectrum in D_2O at 25.0 °C shows broad, featureless peaks in the methylene region, in contrast to the other three carbonate complexes, where sharp peaks and extensive coupling are observed. A similarly

(26) *SAINT*, Version 4; Siemens Analytical X-ray Systems, Inc.: Madison, WI, 1996.
(27) Altomare, A.; Burla, M. C.; Camalli, M.; Cascarano, G. L.; Giacovazzo, C.; Guagliardi, A.; Moliterni, A. G. G.; Polidori, G.; Spagna, R. *J. Appl. Crystallogr.* **1999**, *32*, 115−119.
(28) Farrugia, L. J. *J. Appl. Crystallogr.* **1999**, *32*, 837−838.
(29) Sheldrick, G. M.; Schneider, T. R. *Methods Enzymol.* **1997**, *277*, 319−343.
(30) Reitsma, D. A.; Keene, F. R. *J. Chem. Soc., Dalton Trans.* **1993**, 2859−2860.
(31) Fanshawe, R. L.; Blackman, A. G.; Clark, C. R. *Inorg. Chim. Acta* **2003**, *342*, 114−124.
(32) McClintock, L. F.; Blackman, A. G. Unpublished results.

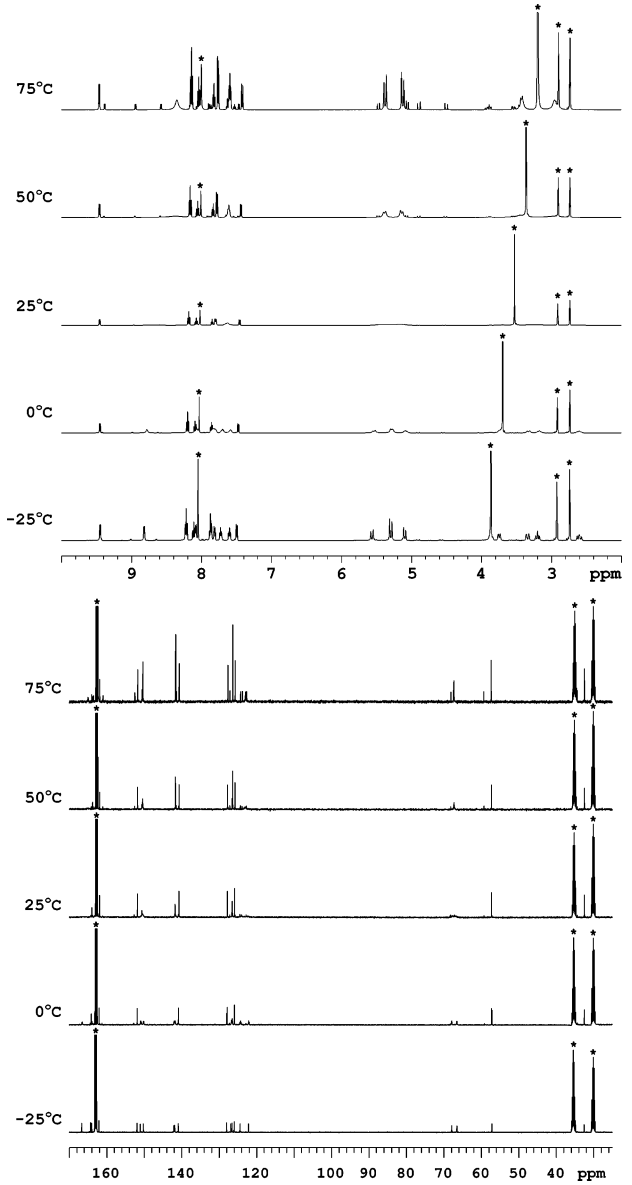

Figure 3. Variable-temperature ^{1}H (top) and ^{13}C (bottom) NMR of [Co(pmea)(O_2CO)]ClO_4 recorded in DMF-d_7. Residual solvent peaks are labeled with an asterisk.

broad peak is also observed in the pyridyl region at approximately 8.7 ppm, while other peaks in this region are again sharp and well-resolved. The ^{13}C NMR spectrum at this temperature shows two peaks at 32.0 and 57.1 ppm, which are assigned to the methylene carbons of the pyridylethyl arm by comparison with the chemical shifts of the analogous carbon atoms in [Co(tepa)(O_2CO)]ClO_4 (peaks at 55.4, 53.6, 31.9, and 31.5 ppm). However, the single peak expected around 70 ppm due to the methylene carbons of the pyridylmethyl arms (the analogous peaks in [Co(tpa)-(O_2CO)]ClO_4 are observed at 72.0 and 72.3 ppm) is not present, and the spectrum is essentially flat in this region. Figure 3 shows variable-temperature ^{1}H and ^{13}C spectra recorded in DMF-d_7 over the temperature range −25.0 to 75.0 °C, and these are consistent with inversion of the six-membered chelate ring about a pseudo-mirror plane containing the carbonate ligand (Figure 4). At −25.0 °C, the six-membered chelate ring is essentially static, thus rendering

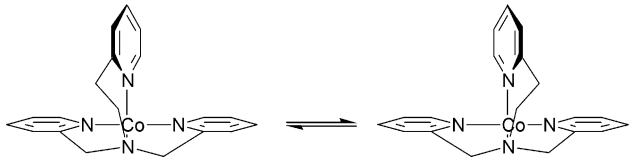

Figure 4. Fluxional ring-inversion process in [Co(pmea)(O_2CO)]$^+$. The chelated carbonate ligand is omitted for clarity.

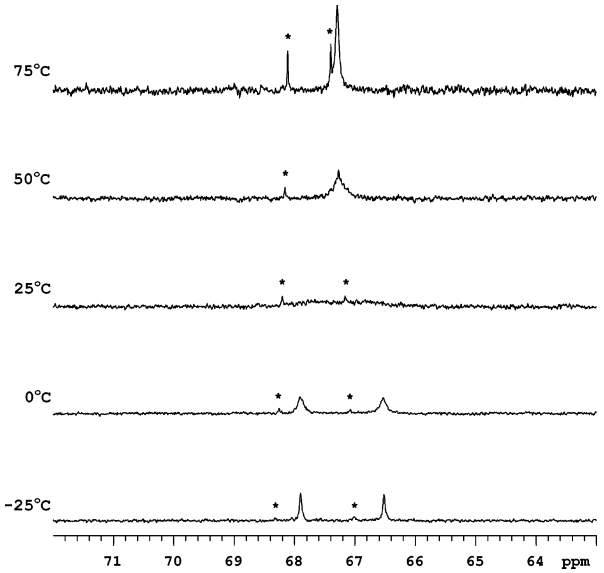

Figure 5. Variable-temperature ^{13}C NMR spectra of [Co(pmea)(O_2CO)]-ClO_4 in DMF-d_7 showing the signals due to the methylene carbon atoms of the pyridylmethyl arms. Peaks marked with an asterisk are due to the 5-isomer.

the pyridylmethyl arms inequivalent and leading to the observation of 10 signals assignable to the 12 pyridyl protons and 7 signals assignable to the 8 methylene protons in the ^{1}H spectrum, and 20 individual peaks in the ^{13}C NMR spectrum.[33] Of particular note is the observation of two peaks at 67.9 and 66.5 ppm (Figure 5), which are due to the inequivalent methylene carbon atoms of the pyridylmethyl arms, while the attached protons appear as two pairs of doublets, the inner legs of which overlap. The observation of 15 ^{13}C signals in five groups of three in the pyridyl region further attests to the inequivalence of all three pyridyl rings at this temperature. As the temperature is increased to 25.0 °C, significant broadening and eventual coalescence of some peaks is evident in both the ^{1}H and ^{13}C spectra. Further heating results in sharpening of the broadened peaks until at 75 °C the methylene protons of the pyridylmethyl arm appear as a doublet of doublets in the ^{1}H spectrum, and the associated carbon atoms now appear as a single peak at 67.3 ppm (Figure 5). Treatment of the ^{13}C data in Figure 5 by the usual method[34] gives $k = 386$ s^{-1} for the inversion process at 25 °C, which corresponds to $\Delta G^{\ddagger} = 58$ kJ mol^{-1} at this temperature. Given that $\Delta G^{\ddagger}$ for the analogous reaction of some five-membered amine chelate rings around room temperature is of the order of 40 kJ mol^{-1},[35] this is a

(33) A small amount of the 5-isomer is also seen in both the ^{1}H and ^{13}C spectra.
(34) Sandström, J. *Dynamic NMR Spectroscopy*; Academic Press: London, 1982.
(35) Hawkins, C. J.; Palmer, J. A. *Coord. Chem. Rev.* **1982**, *44*, 1−60.

Table 1. UV−Vis Data for the Carbonate Complexes

complex	λ_{max}/nm	ϵ/(mol^{-1} L cm^{-1})	λ_{max}/nm	ϵ/(mol^{-1} L cm^{-1})	Δ^a/cm^{-1}
$[Co(tpa)(O_2CO)]^+$	487	192	348	200	22 172
$[Co(pmea)(O_2CO)]^+$	500	180	357	209	21 599
$[Co(pmap)(O_2CO)]^+$	515	140	360	189	21 077
$[Co(tepa)(O_2CO)]^+$	526	102	384	163	20 425

[a] Calculated using the method of Bramley et al.[45] assuming $C = 4B$.

surprisingly large activation barrier to inversion of a six-membered amine chelate ring and must, at least in part, arise from the conformational constraints imposed by the remaining two five-membered chelate rings in the complex. The presence of pyridyl rings requires four of the atoms in each of these five-membered chelate rings to be essentially coplanar (torsion angles of 5.7 and 3.6° for these atoms in the respective chelate rings) and results in envelope conformations[36] in which the tertiary aliphatic nitrogen atom lies out of the plane of the other four atoms. Inspection of Dreiding models shows that these five-membered chelate rings are absolutely rigid. Hence, the large amount of ring strain present in the planar transition state for inversion of the six-membered chelate ring cannot be relieved by motion elsewhere in the ligand, and this leads to a large activation energy for the inversion process and hence a remarkably rigid six-membered chelate ring. It should be noted that the patterns of the peaks due to the small amount of 5-isomer in the mixture are essentially unchanged over the temperature range studied, as the pseudo-mirror plane is absent in this isomer and thus the ring inversion process cannot make the pyridylmethyl arms equivalent. However, it does appear that the relative amount of the 5-isomer increases slightly but noticeably as the temperature is increased, indicating an isomerization process between the 5- and 6-isomers with a significant activation barrier.

The UV−vis spectra of the four carbonate complexes show the two expected $d-d$ bands corresponding to $^1T_1 \leftarrow {}^1A_1$ and $^1T_2 \leftarrow {}^1A_1$ electronic transitions (Table 1). These are well-resolved for all except the pmea complex, where the higher energy transition appears as a shoulder on a high-intensity charge-transfer band. The complexes exhibit a remarkable diversity of colors both in the solid state and in solution, ranging from orange/yellow for the tpa complex to purple for the tepa complex, as shown in Figure 6. Such behavior is unexpected, as complexes of Co(III) containing four N-donor atoms and two O-donor atoms are usually red or purple, and an orange/yellow color generally signifies the presence of six N-donor atoms. Obviously the different colors reflect the different ligand field strengths of the four tripodal ligands, with tpa and tepa exerting the strongest and weakest ligand fields, respectively. Δ values (Table 1) for these complexes show a 1747 cm^{-1} difference in Δ between the tpa and tepa complexes, thus supporting this proposition. Similarly, the large decrease in ϵ values across the series of carbonate complexes suggests increasingly poor metal−ligand orbital overlap as the number of six-membered chelate

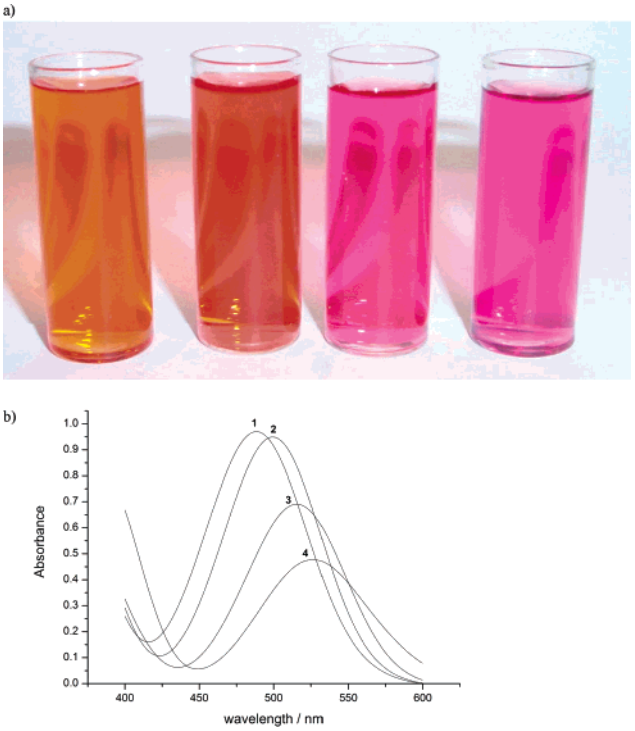

Figure 6. (a) Aqueous solutions (5.0×10^{-3} mol L^{-1}) of (from left to right) $[Co(tpa)(O_2CO)]^+$, $[Co(pmea)(O_2CO)]^+$, $[Co(pmap)(O_2CO)]^+$, and $[Co(tepa)(O_2CO)]^+$. (b) UV−vis spectra of these solutions: $[Co(tpa)(O_2CO)]^+$ (1); $[Co(pmea)(O_2CO)]^+$ (2); $[Co(pmap)(O_2CO)]^+$ (3); $[Co(tepa)(O_2CO)]^+$ (4).

rings in the complexes increases, and this is manifested in increased Co−O and Co−N bond lengths observed across the series $[Co(tpa)(O_2CO)]^+ \rightarrow [Co(tepa)(O_2CO)]^+$ (see below). Similar, but somewhat less pronounced, trends have been observed in the UV−vis spectra of another homologous series of carbonate complexes which contain the aliphatic analogues of the pyridyl ligands discussed herein, comprising $[Co(tren)(O_2CO)]^+$ ($\lambda_{max} = 504$ nm, $\epsilon = 122$ mol^{-1} L cm^{-1}), $[Co(baep)(O_2CO)]^+$ ($\lambda_{max} = 508$ nm, $\epsilon = 107$ mol^{-1} L cm^{-1}), $[Co(abap)(O_2CO)]^+$ ($\lambda_{max} = 524$ nm, $\epsilon = 124$ mol^{-1} L cm^{-1}),[32] and $[Co(trpn)(O_2CO)]^+$ (trpn = tris(3-aminopropyl)-amine) ($\lambda_{max} = 532$ nm, $\epsilon = 125$ mol^{-1} L cm^{-1}).[37] However, the range of λ_{max} values is smaller, and no dramatic reduction in ϵ values across the series is observed, the latter presumably due to the fact that the aliphatic tripodal ligands are less sterically constrained than their pyridyl congeners.

All four carbonate complexes undergo an irreversible one-electron reduction in MeCN solution, with the $E_{red.}$ values (versus decamethylferrocene) of −0.244 V ($[Co(tepa)(O_2CO)]^+$), −0.444 V ($[Co(pmap)(O_2CO)]^+$), −0.535 V ($[Co(pmea)(O_2CO)]^+$), and −0.541 V ($[Co(tpa)(O_2CO)]^+$) showing that the nature of the tripodal ligand significantly influences the redox properties of the complexes. $[Co(tepa)(O_2CO)]^+$ is the easiest to reduce, and this agrees with previous qualitative observations concerning this complex, where removal of the carbonate ligand in 6 M HCl leads to rapid reduction to Co(II).[15] Likewise, this is also consistent with the aforementioned lack of reactivity of a solution of

(36) Hawkins, C. J. *Absolute Configuration of Metal Complexes*; Wiley-Interscience: New York, 1971.

(37) Massoud, S. S.; Milburn, R. M. *Inorg. Chim. Acta* **1988**, *154*, 115−119.

Table 2. Crystal Data and Structure Refinement for the Carbonate Chelates

complex	$[Co(tpa)(O_2CO)]ClO_4 \cdot H_2O$	$[Co(pmea)(O_2CO)]ClO_4 \cdot 3H_2O$	$[Co(pmap)(O_2CO)]ClO_4$	$[Co(tepa)(O_2CO)]ClO_4$
empirical formula	$C_{19}H_{18}ClCoN_4O_8$	$C_{20}H_{20}ClCoN_4O_{10}$	$C_{21}H_{22}ClCoN_4O_7$	$C_{22}H_{24}ClCoN_4O_7$
fw	524.76	570.78	536.81	550.83
T/K	168(2)	168(2)	163(2)	161(2)
λ/Å	0.71073	0.71073	0.71069	0.71073
space group	$P\bar{1}$	$P\bar{1}$	$C2/c$	$Pbca$
a/Å	8.174(1)	8.339(4)	17.717(5)	14.8650(15)
b/Å	15.558(2)	9.808(4)	18.089(5)	14.8578(14)
c/Å	17.073(2)	15.627(7)	14.569(5)	20.474(2)
α/deg	80.94(6)	73.357(6)		
β/deg	77.40(6)	78.666(6)	109.892(5)	
γ/deg	77.05(6)	85.522(6)		
V/Å^3	2051.5(8)	1200.4(9)	4391(2)	4522.0(8)
Z	4	2	8	8
D_c/(Mg m^{-3})	1.699	1.579	1.624	1.618
μ/mm^{-1}	1.025	0.889	0.956	0.931
final R indices [$I > 2\sigma(I)$]	R1 = 0.1158, wR2 = 0.2828	R1 = 0.0557, wR2 = 0.1452	R1 = 0.0473, wR2 = 0.1131	R1 = 0.0621, wR2 = 0.1218
R indices (all data)	R1 = 0.2528, wR2 = 0.3605	R1 = 0.0901, wR2 = 0.1591	R1 = 0.0513, wR2 = 0.1149	R1 = 0.0697, wR2 = 0.1247

Co(II) and tepa toward aerial oxidation. Such observations parallel those of Karlin and co-workers, who found that the Cu(I) complexes of tpa, pmea, pmap, and tepa, displayed differing reactivities toward O_2, with $[Cu(tepa)]^+$, in contrast to the other three complexes, being completely unreactive toward O_2.[23] Similar trends in the electrochemical behavior to those observed here were also reported for the Cu(II) complexes $[Cu(L)Cl]^+$, with potentials for the four complexes ranging over 501 mV, and with $[Cu(tepa)Cl]^+$ displaying the most positive reduction potential.

^{59}Co NMR data on the four complexes also show that the nature of the tripodal ligand affects the amount of electron density at the Co nucleus, with chemical shifts for the four complexes of 10121 ppm ($[Co(tepa)(O_2CO)]^+$), 9096 ppm ($[Co(pmap)(O_2CO)]^+$), 8509 ppm ($[Co(pmea)(O_2CO)]^+$), and 7965 ppm ($[Co(tpa)(O_2CO)]^+$) in D_2O solution. Such a large variation in chemical shift across a series of complexes having identical donor atoms and differing only in the size of the chelate rings is surprising. Gahan and co-workers found a variation of ca. 830 ppm across a series of Co(III) complexes of hexadentate N_4S_2 ligands containing chelate rings of varying size, while other data tabulated in the same paper show comparatively small variations in chemical shifts (maximum of ~1100 ppm) across individual series of complexes with N_6, N_5S, N_4S_2, and N_3S_3 donor sets.[38] Complexes having N_4O_2 donor sets typically display resonances in the range 9000−10 000 ppm,[39] while the chemical shift of 7965 ppm observed for $[Co(tpa)(O_2CO)]^+$ is in the upper end of the range of values more typical of complexes containing an N_6 donor set,[40] further serving to emphasize the ligand field strength of the tpa ligand. Again, a similar, but less pronounced, trend is seen for $[Co(tren)(O_2CO)]^+$ (8450 ppm), $[Co(baep)(O_2CO)]^+$ (8728 ppm), and $[Co(abap)(O_2CO)]^+$ (9177 ppm),[32] confirming the utility of using ^{59}Co NMR as a probe of ligand field strength. Although the predicted[41,42] linear relationship between the Co magnetogyric ratio and the wavelength of the lowest energy absorption band exists for the four carbonate complexes (a plot of γ versus $1/\Delta E$ is linear with $R^2 = 0.965$, Figure S1 of the Supporting Information), the y intercept of 9.92 MHz T^{-1}, which corresponds to $\gamma_o(^{59}Co)$, the magnetogyric ratio of the bare Co nucleus, is significantly lower than previously reported values, which range consistently around 10.04−10.05 MHz T^{-1}. Inclusion of an intercept of this magnitude in the data set reduces R^2 to 0.76, while incorporation of β, the nephelauxetic parameter,[43−45] worsens the fit noticeably. As the complexes in question deviate significantly from octahedral symmetry, such behavior is perhaps to be expected, given the assertion of Bramley and co-workers that "*not much confidence should be placed in* $\gamma_o(^{59}Co)$ *values found by extrapolation from nonorthoaxial data*".[45]

X-ray Crystallography. X-ray data for the four carbonate complexes are summarized in Table 2, while Table 3 details Co−N and Co−O bond length data for these complexes. Figure 7 gives ORTEP diagrams of the cations. In all cases, the structures consist of a Co(III) ion coordinated to all four N-donor atoms of the tripodal ligand, with the remaining two coordination sites occupied by O atoms of the chelating carbonate ligand to give a distorted octahedral environment about the metal ion. In all but the tepa complex, the Co−N bond to the aliphatic tertiary N atom is significantly longer than those to the pyridine N atoms, as has been found previously in complexes containing tripodal pyridyl-based ligands.[46] The angle subtended by the chelating carbonate ligand remains essentially invariant at 69.5 ± 0.5° as the tripodal ligand varies, and there is relatively little difference in the dimensions of the carbonate chelate rings of the four complexes. The largest changes across the series of complexes are observed in the bond distances and angles

(38) Sharrad, C. A.; Cavigliasso, G. E.; Stranger, R.; Gahan, L. R. *Dalton Trans.* **2004**, 767−777.
(39) Kidd, R. G.; Goodfellow, R. J. The Transition Metals. In *NMR and the Periodic Table*, Chapter 8; Harris, R. K., Mann, B. E., Eds.; Academic Press: London, 1978.
(40) Hendry, P.; Ludi, A. *Adv. Inorg. Chem.* **1990**, *35*, 117−198.
(41) Griffith, J. S.; Orgel, L. E. *Trans. Faraday Soc.* **1957**, *53*, 601−606.
(42) Freeman, R.; Murray, G. R.; Richards, R. E. *Proc. R. Soc. London* **1957**, *A242*, 455−466.
(43) Juranic, N. *Inorg. Chem.* **1980**, *19*, 1093−1095.
(44) Juranic, N. *Inorg. Chem.* **1983**, *22*, 521−525.
(45) Bramley, R.; Brorson, M.; Sargeson, A. M.; Schaeffer, C. E. *J. Am. Chem. Soc.* **1985**, *107*, 2780−2787.
(46) A search of the Cambridge Structural Database (Version 5.25, Updates, July 2004) revealed 49 monomeric six-coordinate transition metal complexes containing the tpa ligand. Average M−N distances are 2.111 and 2.083 Å for bonds to the aliphatic tertiary and pyridine N atoms, respectively.

Table 3. Coordination Geometries about the Cobalt(III) Ions in the Carbonate Complexes[a]

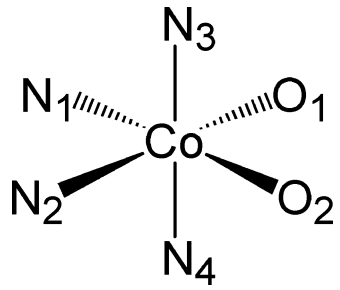

complex	Co−O_1	Co−O_2	Co−N_1	Co−N_2	Co−N_3	Co−N_4
$[Co(tpa)(O_2CO)]^+$ [b]	1.863(8)	1.874(9)	1.925(11)	1.887(10)	1.898(11)	1.911(11)
$[Co(tpa)(O_2CO)]^+$	1.876(9)	1.865(9)	1.947(11)	1.869(10)	1.880(12)	1.889(13)
$[Co(pmea)(O_2CO)]^+$	1.893(3)	1.912(3)	1.942(4)	1.958(3)	1.888(4)	1.916(3)
$[Co(pmap)(O_2CO)]^+$	1.902(2)	1.904(2)	1.994(3)	1.977(3)	1.947(3)	1.927(3)
$[Co(tepa)(O_2CO)]^+$	1.892(2)	1.928(2)	2.008(3)	1.991(3)	1.968(3)	2.012(3)

[a] N_1 corresponds to the tertiary N atom of the tripodal ligand in all cases. Note that there are two independent molecules in the asymmetric unit of $[Co(tpa)(O_2CO)]ClO_4 \cdot H_2O$. [b] Note the caveat concerning quantitative data for this complex given in the Experimental Section.

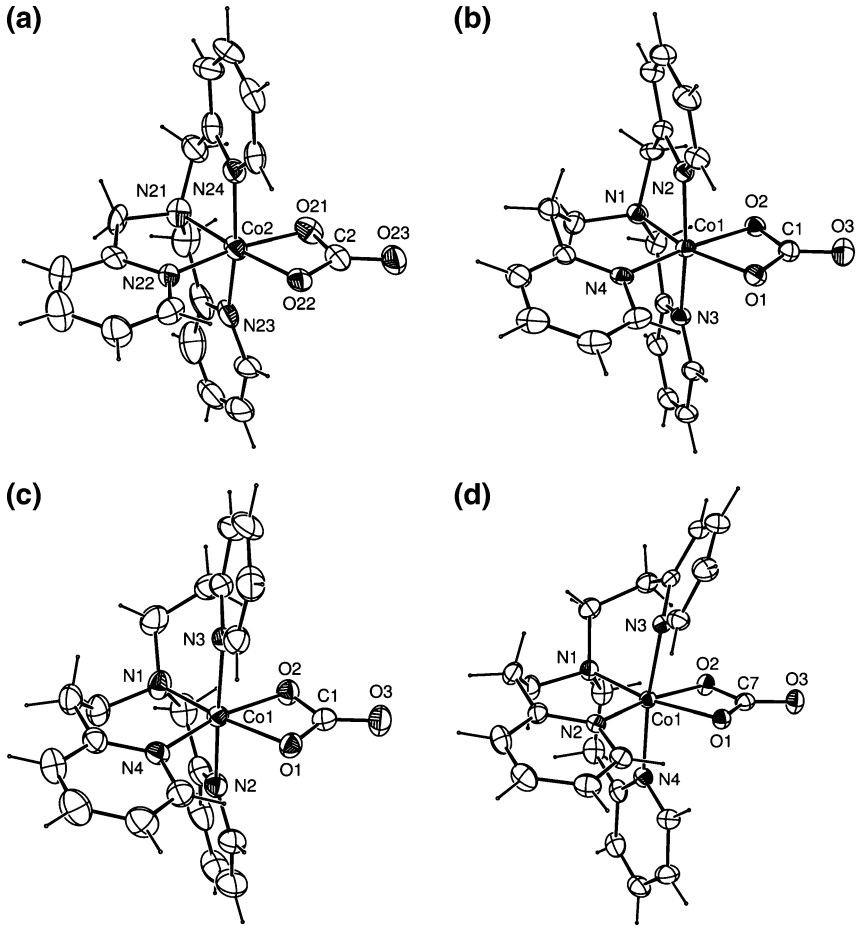

Figure 7. ORTEP diagrams of the cations $[Co(tpa)(O_2CO)]^+$ (a), $[Co(pmea)(O_2CO)]^+$ (b), $[Co(pmap)(O_2CO)]^+$ (c), and $[Co(tepa)(O_2CO)]^+$ (d). Only one of the two independent molecules in the asymmetric unit of $[Co(tpa)(O_2CO)]ClO_4 \cdot H_2O$ is shown. Thermal ellipsoids are drawn at the 50% probability level.

contained in the primary coordination sphere of the Co(III) ions. As outlined in Table 3, there is a gradual increase in the Co−O and, particularly, Co−N bond lengths as the number of six-membered chelate rings in the complexes increase, with the difference in the average Co−N bond length between the tpa and tepa complexes approaching 0.1 Å. This contrasts with the ∼0.01 Å difference in average Co−N bond length observed in the series of complexes $[Co(en)_3]^{3+}$, $[Co(en)_2(tn)]^{3+}$, and $[Co(tn)_3]^{3+}$, (tn = 1,3-diaminopropane),[47] implying that the structural constraints inherent in the tripodal pyridyl ligands place substantial

(47) $[Co(en)_3]^{3+}$, 1.967 Å. Average of 28 structural determinations having $R_1 < 0.05\%$. Λ-$[Co(en)_2(tn)]Br_3$, 1.972 Å. Schousboe-Jensen, H. V. F. *Acta Chem. Scand.* **1972**, *26*, 3413−3420. Λ-$[Co(tn)_3]Cl_3 \cdot H_2O$, 1.979 Å. Nagao, R.; Marumo, F.; Saito, Y. *Acta Crystallogr.* **1973**, *B29*, 2438−2443.

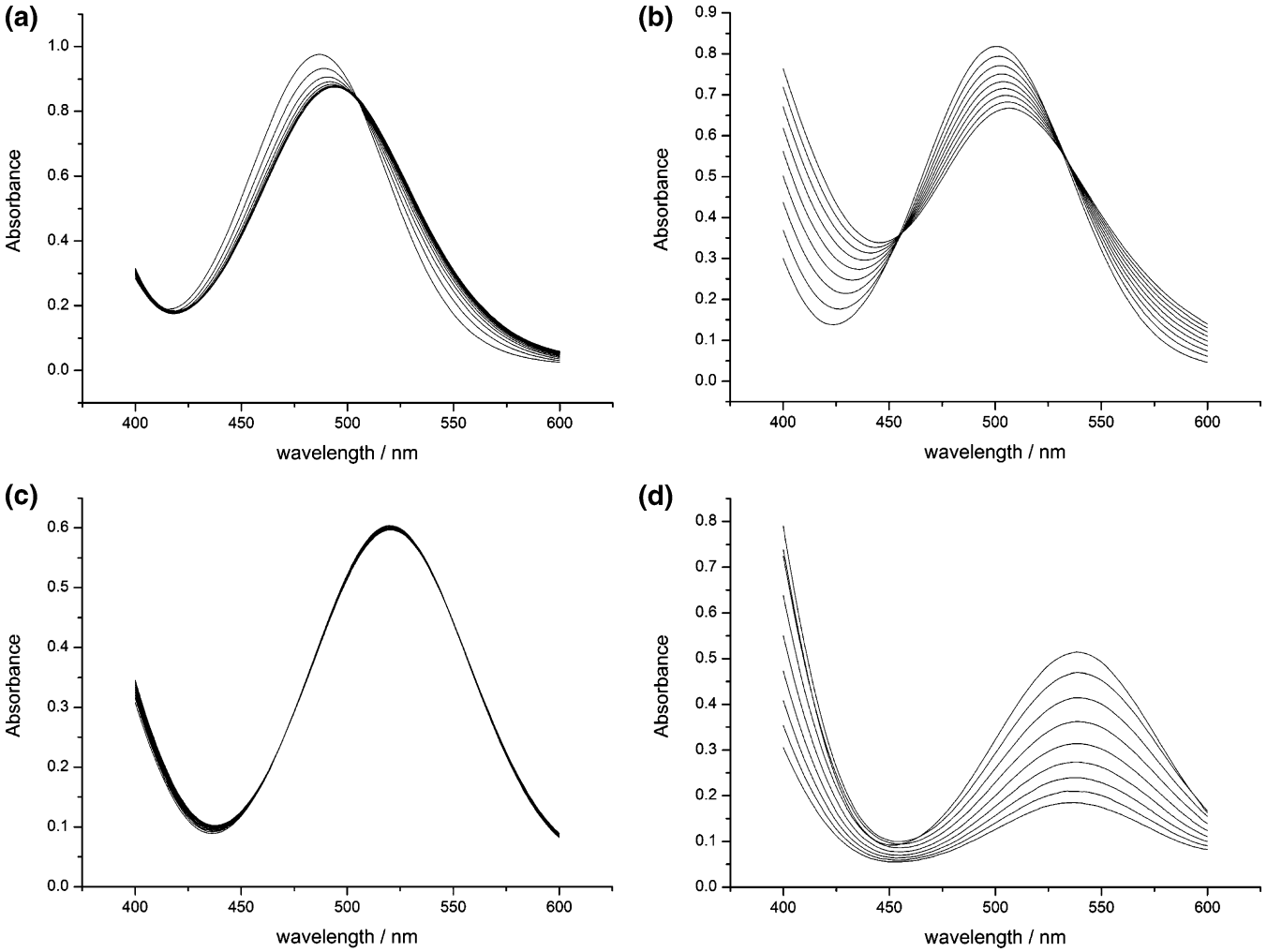

Figure 8. Repetitive-scan visible spectra of $[Co(tpa)(O_2CO)]^+$ (a), $[Co(pmea)(O_2CO)]^+$ (b), $[Co(pmap)(O_2CO)]^+$ (c), and $[Co(tepa)(O_2CO)]^+$ (d) in 6 M HCl. The collection time is 4 h, and the time between spectra is 30 min for all but $[Co(tpa)(O_2CO)]^+$, where the collection time is 32 min and the time between spectra is 4 min. Absorbance decreases at λ_{max} are observed in all cases.

limitations on the positioning of the donor atoms about the metal ion. Hence, the significant lengthening of the Co−N and Co−O bonds in the tripodal pyridyl complexes obviously leads to a weaker ligand field through poorer overlap of the metal and ligand orbitals, and this is consistent with both the shift of λ_{max} to longer wavelengths and the concomitant decrease in ϵ observed as the number of six-membered chelate rings in the complexes is increased. Such an argument can also be used to provide a rationalization of the UV−vis, electrochemical, and ^{59}Co NMR observations discussed above.

Bicarbonate Complexes. The carbonate complexes all show extraordinary stability toward hydrolysis in acidic aqueous solution. Figure 8 shows repetitive scan visible spectra of the four carbonate complexes in 6 M HCl, and it can be seen that all four complexes exhibit substantial stability in the highly acidic medium, hydrolyzing slowly to give (presumably) the diaqua species for all but the tepa complex, which gives $Co^{2+}(aq)$.[48] The tpa complex reacts most rapidly, hydrolyzing essentially completely over a period of ∼30 min under these conditions, with $k_{obs} = 2.14 \times 10^{-3}$ s^{-1}. This compares with k_{obs} values for $[Co(tren)(O_2CO)]^+$, $[Co(NH_3)_4(O_2CO)]^+$, and $[Co(N\text{-}Mecyclen)(O_2CO)]^+$ of 3.36, 1.44, and 5.49×10^{-3} s^{-1} under the same conditions of $[H_3O^+]$.[13,49] Both the tepa and pmea complexes hydrolyze much more slowly ($k_{obs} = 7.17 \times 10^{-5}$ and 3.67×10^{-5} s^{-1}, respectively) while the pmap complex shows extraordinary stability, with only a minimal absorbance decrease at λ_{max} over 4 h. All four complexes are remarkably slow to hydrolyze when compared to the majority of Co(III) carbonate chelate complexes that have been studied, which have half-lives for ring opening of the carbonate ring ranging from ∼0.008 to 90 s.[13,50] This unusual inertness of chelated carbonate toward acid parallels that observed for $[Co(py)_4(O_2CO)]^+$ which shows no reaction in 12 M HCl over 10 min,[14] and also that of $[Co([3^5]adz)(O_2CO)]AsF_6$

(48) Hydrolysis of $[Co(pmea)(O_2CO)]^+$ by prolonged (days) standing in aqueous $HClO_4/NaClO_4$ solution leads to crystallization of $[Co(pmea)(OH_2)_2](ClO_4)_3 \cdot 2H_2O$, which has been characterised as the 6-isomer by X-ray crystallography. McClintock, L. F.; Blackman, A. G. Unpublished results.

(49) The quoted k_{obs} values are calculated from the data given in ref 13 for $I = 1.0$ M and should thus be considered approximate.

(50) The four complexes do not show similar unusual stability in aqueous alkaline solution. Dissolution of both $[Co(tepa)(O_2CO)]ClO_4$ and $[Co(pmap)(O_2CO)]ClO_4$ in 1.0 M NaOH(aq) gives production of $Co(OH)_2$ within minutes, while the corresponding reaction with $[Co(pmea)(O_2CO)]ClO_4$ and $[Co(tpa)(O_2CO)]ClO_4 \cdot H_2O$ gives what are presumably the dihydroxo complexes, again over a period of minutes.

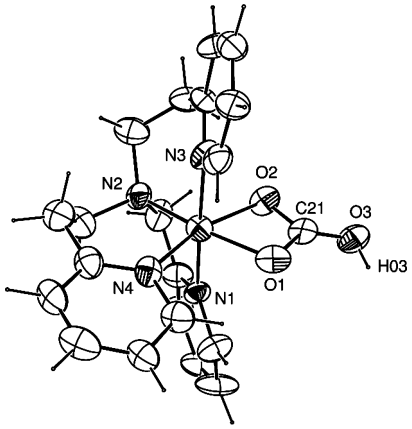

Figure 9. ORTEP diagram of the $[Co(pmap)(O_2COH)]^{2+}$ cation. Thermal ellipsoids are drawn at the 50% probability level.

Table 4. Crystal Data and Structure Refinement for $[Co(pmap)(O_2COH)]ZnCl_4 \cdot 3H_2O$

empirical formula	$C_{21}H_{23}Cl_4CoN_4O_6Zn$
fw	693.53
T/K	173(2)
λ/Å	0.710 73
space group	$P2_12_12_1$
a/Å	7.58(2)
b/Å	17.64(5)
c/Å	20.70(6)
V/Å^3	2766(14)
Z	4
D_c/(Mg m^{-3})	1.665
μ/mm^{-1}	1.896
final R indices [$I > 2\sigma(I)$]	R1 = 0.0878, wR2 = 0.1867
R indices (all data)	R1 = 0.1926, wR2 = 0.2272

(adz = [3^5]adamanzane), dissolution of which in 25% HBr yields crystals of the chelated bicarbonate complex over 2 h following addition of Li_2ZnBr_4.[19]

The chelate bicarbonate complexes $[Co(pmea)(O_2COH)]ZnCl_4$ and $[Co(pmap)(O_2COH)]ZnCl_4 \cdot H_2O$ can be isolated from $ZnCl_2$/HCl solutions having $[H_3O^+] = 2.5$ M, while $[Co(pmap)(O_2COH)]ZnBr_4 \cdot 2H_2O$ crystallizes in an analogous fashion from a $ZnBr_2$/HBr solution. Although $[Co(tpa)(O_2COH)]^+$ is undoubtedly formed on dissolution of $[Co(tpa)(O_2CO)]ClO_4$ in aqueous acidic solution, no crystalline material could be isolated, presumably due to the relatively rapid hydrolysis of the carbonate complex.

The X-ray structure of $[Co(pmap)(O_2COH)]ZnCl_4 \cdot 3H_2O$ confirms the presence of a chelated bicarbonate ligand. X-ray data for this complex are given in Table 4, and an ORTEP diagram of the cation is given in Figure 9. The complex crystallizes as the 6-isomer, showing that isomerization of the starting carbonate complex does not occur in aqueous acidic solution. O3, the *exo* oxygen atom of the chelated bicarbonate, is H-bonded to a water of crystallization, with the O3−H03−O4 angle being nearly linear, strongly suggesting this, rather than either of the *endo* oxygen atoms, as the site of protonation. Dissolution of $[Co(pmap)(O_2CO)]ClO_4$ in less acidic solution than above (1.8 M $HClO_4$/0.9 M $NaClO_4$) in the presence of only ClO_4^- as counterion results in the unexpected isolation of $[Co(pmap)(O_2COH)][Co(pmap)(O_2CO)](ClO_4)_3$, which contains a 1/1 mixture of the chelated carbonate and bicarbonate cations. This formulation was made initially on the basis of microanalytical data, which were inconsistent with formation of the expected bicarbonate complex $[Co(pmap)(O_2COH)](ClO_4)_2$, and a poor-quality X-ray crystal structure[51] confirmed the presence of both carbonate and bicarbonate cations in the crystalline material, with an H-bonding interaction between the *exo* oxygen atoms of neighboring carbonate and bicarbonate chelate rings ($d_{O-O} = 2.405$ Å).

Structural Basis of Acid Stability. The stability of these carbonate complexes in acidic solution is remarkable, and obviously the ancillary tripodal ligands play a substantial role in determining the reactivity of these complexes toward acid. However, the electronic effects exerted by the pyridyl tripodal ligands are unlikely to be responsible for the stability of their cobalt(III) carbonate complexes toward acid, as we have shown above that the four pyridyl ligands studied exert very different ligand fields which in turn lead to systematic trends in the spectroscopic and electrochemical properties of the complexes which are not mirrored in the reactivity of the complexes toward acid. This is in accord with the views of Buckingham and Clark, who proposed that protonation of an *endo* oxygen atom is the mechanistically important step that leads to dechelation and that the steric, rather than electronic, nature of the ancillary ligand(s) around the Co(III) ion influences the extent to which either of these oxygen atoms is protonated and hence the rate of chelate ring opening. The X-ray structural data reported in this and other papers now lend support to this proposal. Figure 10 shows space-filling diagrams of the cations of the carbonate complexes studied herein and, in addition, the cations of two other structurally characterized complexes $[Co([3^5]adz)(O_2CO)]AsF_6$[19] and $[Co(py)_4(O_2CO)]ClO_4 \cdot H_2O$,[52] which are similarly slow to hydrolyze, while Figure 11 shows similar diagrams of the cations $[Co(NH_3)_4(O_2CO)]^+$,[53] $[Co(en)_2(O_2CO)]^+$,[54] $[Co(tren)(O_2CO)]^+$,[55] and $[Co(nta)(O_2CO)]^{2-}$,[56] all of which hydrolyze rapidly in acidic solution. Figure 10 clearly shows that while the *exo* oxygen atom of the carbonate ligand is free of steric encumbrance in all cases, the tpa, pmea, pmap, tepa, [3^5]adz, and $(py)_4$ ancillary ligands provide significant impediments to protonation of the *endo* oxygen atoms from either side in the plane of the carbonate ligand and also to proton transfer from the *exo* oxygen atom, a process that would almost certainly be solvent assisted. In

(51) While excellent X-ray data were collected for this complex ($R_{int} = 0.0453$, $R_{sigma} = 0.0373$) and a sensible solution could be obtained, refinement showed the presence of extensive disorder in both independent cations of the asymmetric unit. This took the form of rotational disorder about the tertiary aliphatic N atom of the pmap ligand, resulting in superimposed six- and five-membered chelate rings in each cation. Extensive attempts to resolve this disorder were unsuccessful, with numerous atoms displaying nonpositive definite thermal parameters. However, isotropic refinement of all but the Co, Cl, and perchlorate O atoms gave $R_1 = 0.0779$% with the carbonate/bicarbonate portions of both cations being well-resolved.

(52) Kaas, K.; Sørensen, A. M. *Acta Crystallogr.* **1973**, *B29*, 113−120.
(53) Bernal, I.; Cetrullo, J. *Struct. Chem.* **1990**, *1*, 227−234.
(54) García-Granda, S.; Calvo-Pérez, V.; Gómez-Beltrán, F. *Acta Crystallogr.* **1993**, *C49*, 322−324.
(55) Düpre, Y.; Bartscherer, E.; Maas, O.; Sander, J.; Hegetschweiler, K. *Z. Kristallogr.* **1999**, *214*, 405−406.
(56) Visser, H. G.; Purcell, W.; Basson, S. S. *Polyhedron* **2001**, *20*, 185−190.
(57) Fanshawe, R. L.; Clark, C. R.; Blackman, A. G. *Acta Crystallogr.* **2001**, *E57*, m17−m18.

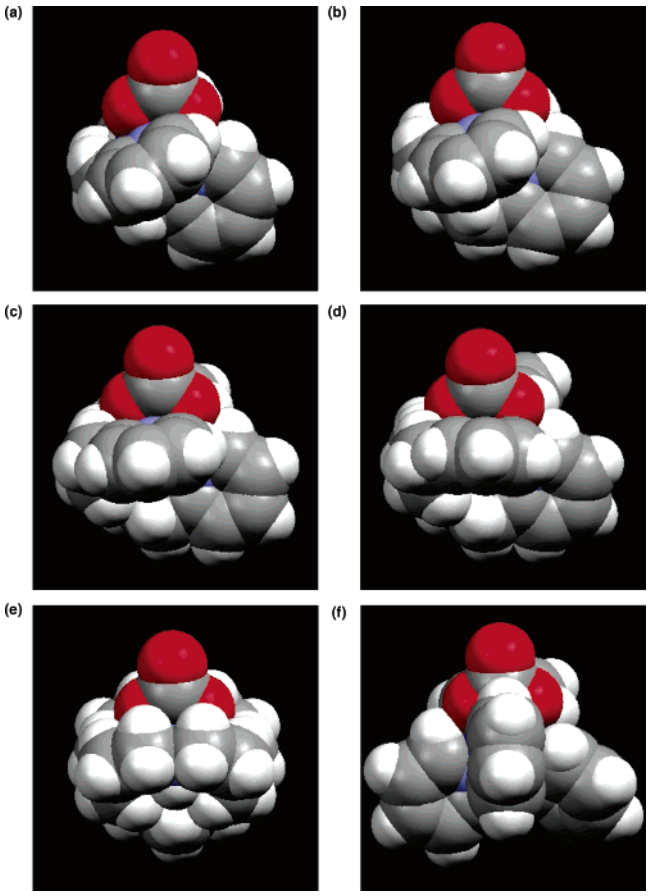

Figure 10. Space-filling diagrams of $[Co(tpa)(O_2CO)]^+$ (a), $[Co(pmea)(O_2CO)]^+$ (b), $[Co(pmap)(O_2CO)]^+$ (c), $[Co(tepa)(O_2CO)]^+$ (d), $[Co([3^5]adz)(O_2CO)]^+$ (e), and $[Co(py)_4(O_2CO)]^+$ (f).

the case of the pyridyl tripodal ligands, these impediments arise from close approach of the protons α to the aliphatic tertiary nitrogen atom on one side, and the proton α to the coordinated nitrogen atom of the pyridine ring in the plane of the carbonate ligand on the other. This contrasts markedly with the diagrams in Figure 11, in which the carbonate ligand is situated well clear of the ancillary ligand(s) and both *endo* oxygen atoms appear easily accessible. It is interesting to note that the protons alpha to the aliphatic tertiary nitrogen atom of both the tren and nta tripodal ligands are not situated in a similar position to the analogous protons of the pyridyl tripodal ligands and thus do not provide the same steric hindrance.

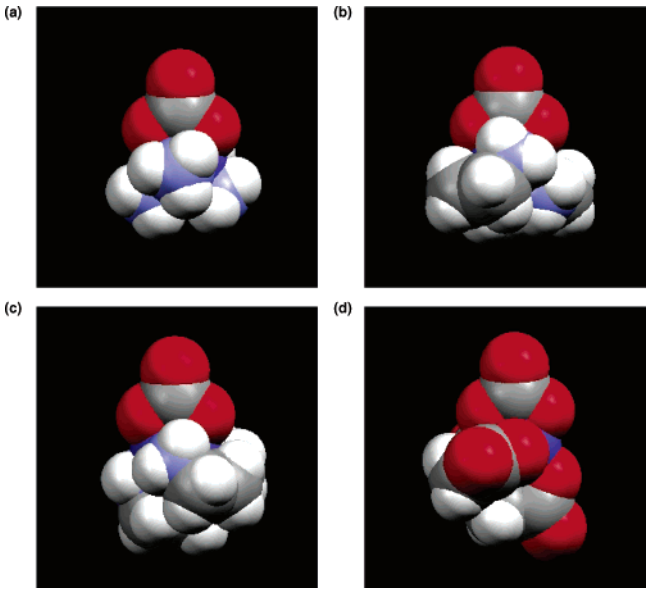

Figure 11. Space-filling diagrams of $[Co(NH_3)_4(O_2CO)]^+$ (a), $[Co(en)_2(O_2CO)]^+$ (b), $[Co(tren)(O_2CO)]^+$ (c), and $[Co(nta)(O_2CO]^{2-}$ (d).

Thus it appears that it is indeed the environment of the *endo* oxygen atoms that determines the reactivity of the chelated carbonate ligand toward acid. With this in mind, we are currently preparing sterically hindered derivatives of pmea and pmap, substituted at the 6-position of the unique pyridyl ring which binds in the same plane as the carbonate ligand. Such ligands should lead to the synthesis of still more stable chelated bicarbonate complexes, which should in turn allow studies of the reactivity of the chelated carbonate ligand toward various substrates under acidic conditions.

Acknowledgment. We thank Professor Ward Robinson and Dr. Jan Wikaira (University of Canterbury) for X-ray data collection. L.F.M. thanks the Foundation for Research, Science and Technology for the award of a Bright Futures Ph.D. Scholarship.

Supporting Information Available: Figure S1, showing plots of γ versus λ_{max} for the carbonate complexes (pdf) and crystallographic data (CIF). This material is available free of charge via the Internet at http://pubs.acs.org.

IC0482537